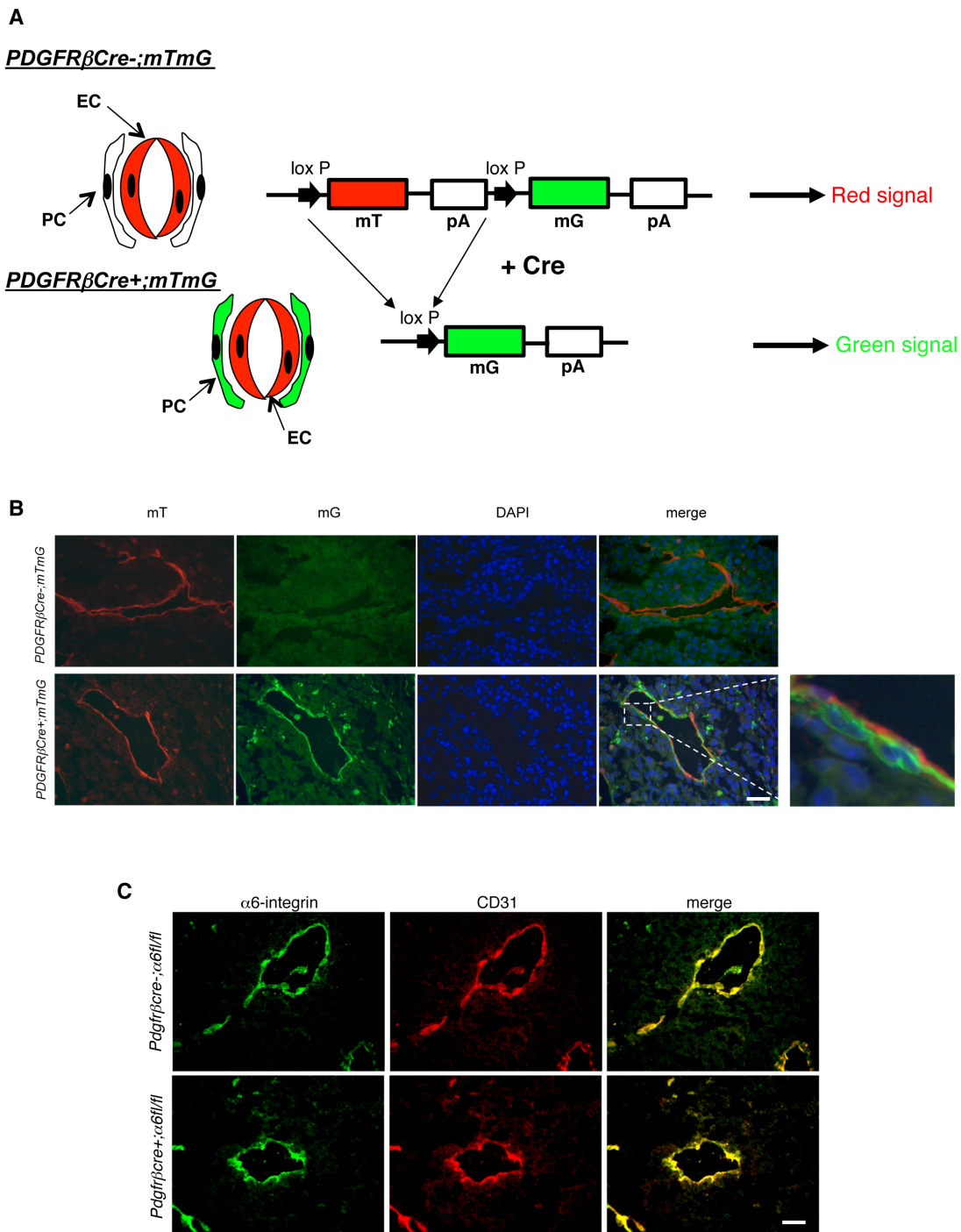


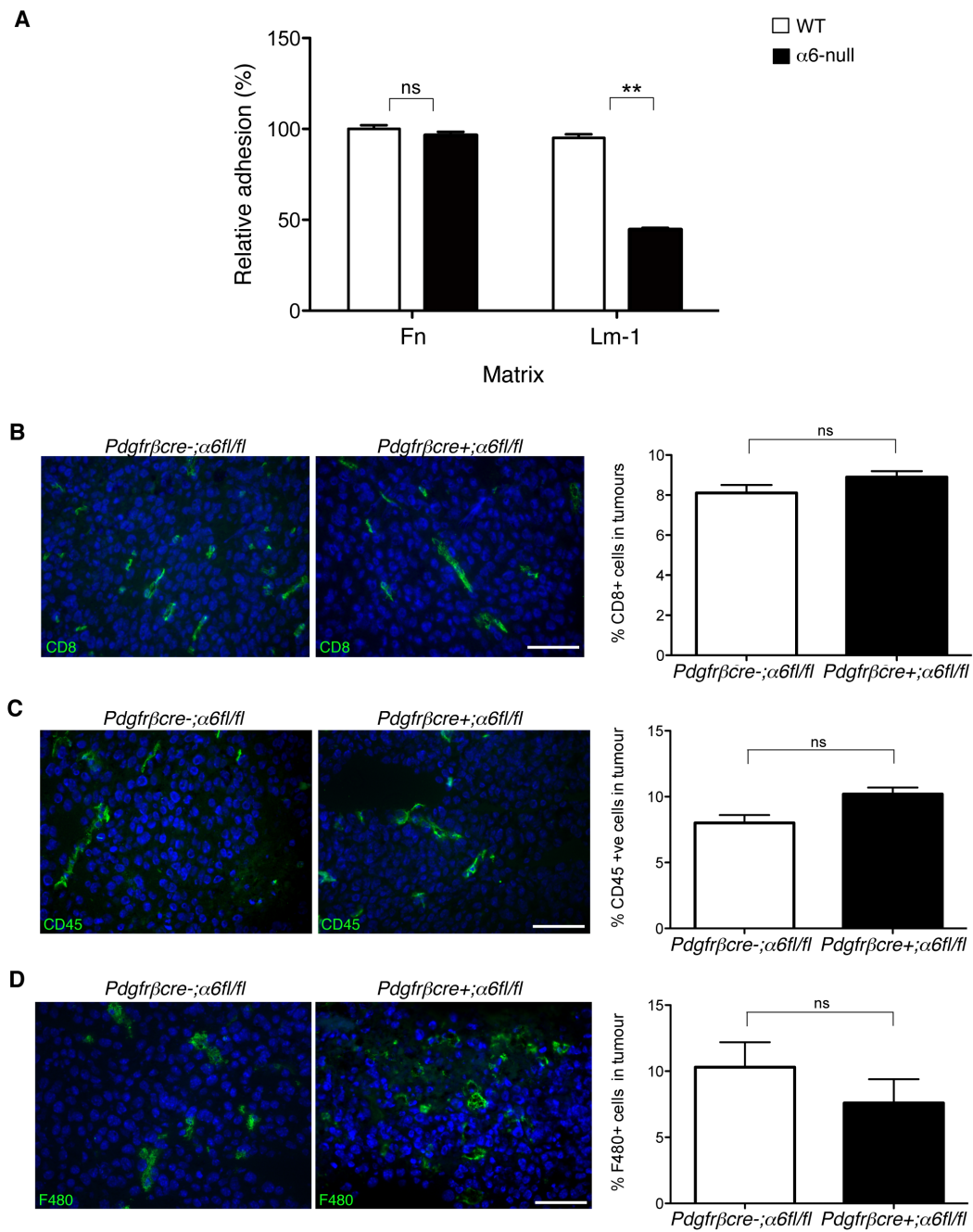
Supplementary Figure 1. Characterisation of *pdgfrβcre-;α6fl/fl* and *pdgfrβcre+;α6fl/fl* mice and morphological analysis of tissue and postnatal retinal angiogenesis. (A) *Pdgfrβcre-;α6fl/fl* mice crossed to *pdgfrβcre+;α6fl/fl* mice produce: litters that had a similar

number of *pdgfr β cre-; α 6fl/fl* and *pdgfr β cre+; α 6fl/fl* mice in predicted Mendelian ratios, **(B)** and similar ratios of *pdgfr β cre+; α 6fl/fl* males and females, identified at weaning. **(C)** Mice were weighed at 3 months old. No differences were observed in the weights of sex-matched mice between the two genotypes. **(D)** All mice were analysed by PCR genotyping and shows a product identifying *pdgfr β cre+* PCR at approx. 1000 bp. α 6-integrin-floxed PCR shows products identifying homozygous α 6-integrin floxed (α 6fl/fl) (154 bp), WT non-floxed (α 6-integrin wt) (120 bp), and heterozygous (α 6-integrin fl/wt) mice (154 bp and 120 bp). **(E)** Representative H&E stained sections of lung, heart, liver and spleen from 12 week old *pdgfr β cre-; α 6fl/fl* and *pdgfr β cre+; α 6fl/fl* mice. No gross morphological defects were observed. **(F)** Representative high power images of blood vessels in lung, heart and liver from *pdgfr β cre-; α 6fl/fl* and *pdgfr β cre+; α 6fl/fl* mice showed no obvious morphological blood vascular defects between the genotypes. **(G)** Confocal microscopy images show 3D Z-stack reconstructions of flat whole-mount immunofluorescent stained retinas from *pdgfr β cre-; α 6fl/fl* and *pdgfr β cre+; α 6fl/fl* mice at postnatal day (P) 9. Arterial, vein and capillary vessels in the superficial retinal plexus are visualised with Isolectin B4 (IB4, green). Pericytes are identified with NG2 (red); n=4 retinas/genotype. Scale bar in **E**=20 μ m; **F**=100 μ m; **G**=50 μ m.



Supplementary Figure 2. mTmG reporter activity in pericytes after PDGFRβCre excision. *mTmG* mice are used as a reporter of Cre activity in Cre⁺ mice. We generated *pdgfrβcre-;mTmG* and *pdgfrβcre+;mTmG* mice. (A) Schematic representation of the mTmG reporter effect in *pdgfrβcre+* mice. In non-Cre expressing cells mT (red) signal is observed in endothelial cells (EC). In Cre expressing cells the mT transgene is excised and the mG

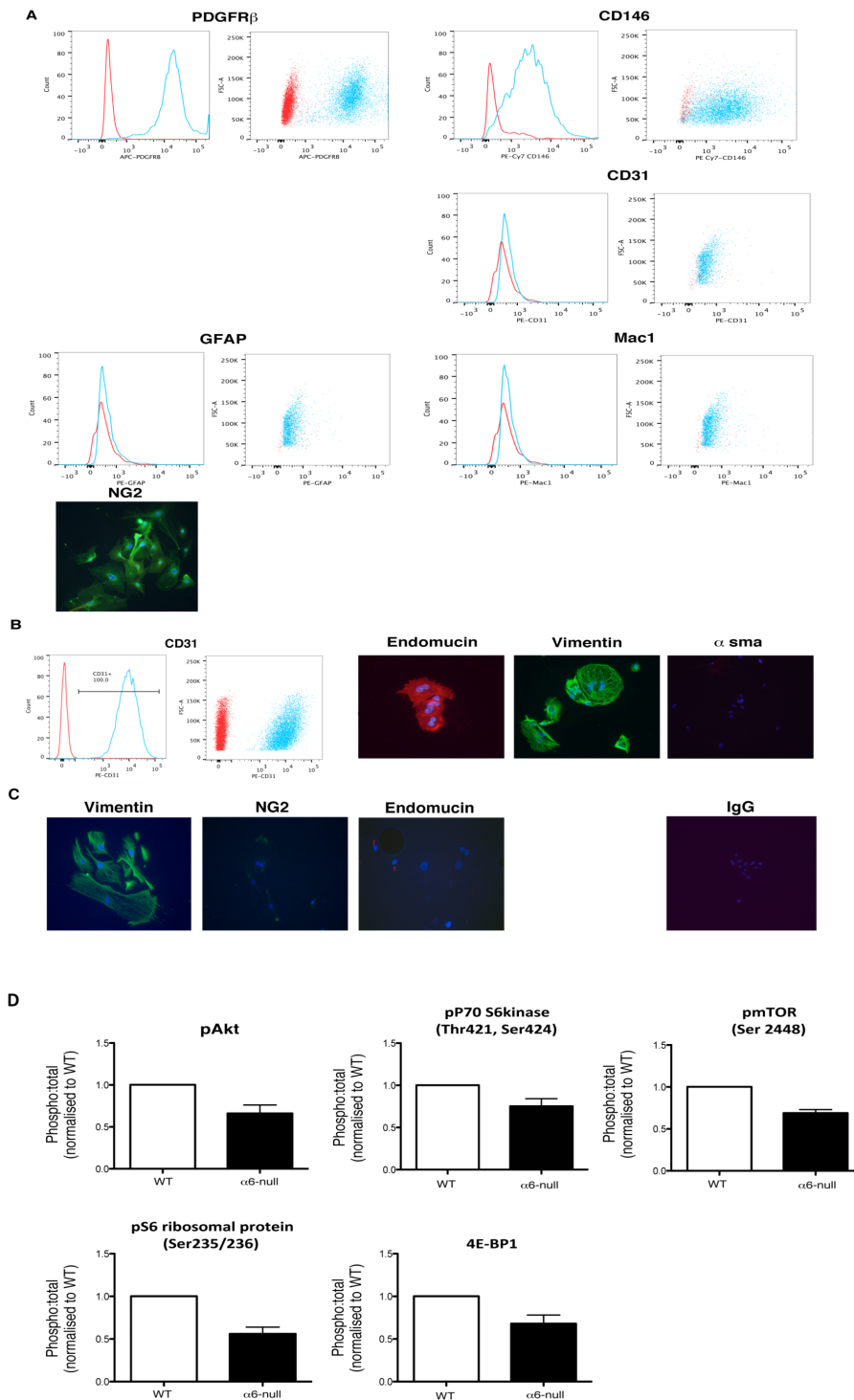
(green) signal is observed in pericytes (PC). **(B)** B16F0 tumour cells were injected subcutaneously into *pdgfr β cre⁻;mTmG* and *pdgfr β cre⁺;mTmG* mice and tumours excised 12 days post inoculation. Tumour blood vessels were examined for expression of both membrane-targeted tandem dimer Tomato (mT) (red), seen in all host tissue and membrane-targeted green fluorescent protein (GFP) (mG) (green). GFP expression was observed only in *pdgfr β cre⁺;mTmG* mice, as expected and almost exclusively in PCs surrounding blood vessels (*white box*, magnified region). **(C)** Tumour blood vessels immunostained with antibodies to α 6-integrin and CD31 revealed co-expression of the 2 markers, showing that α 6-integrin expression is not affected on endothelial cells *in vivo*. Scale bars in **B**, **C** =50 μ m.



Supplementary Figure 3. Adhesion of wild-type and $\alpha 6$ -null pericytes to Laminin-1 and immune cell infiltration in tumours.

(A) 5×10^4 wild-type (WT) and $\alpha 6$ -null mouse brain pericytes were allowed to adhere to Laminin-1 (Lm-1; $10 \mu\text{g/ml}$) and Fibronectin (Fn; $10 \mu\text{g/ml}$) coated 96-well plates for 1 h at

37°C. $\alpha 6$ -null pericytes do not bind effectively to the Lm-1 matrix compared with WT pericytes. No difference in Fn adhesion was observed between WT and $\alpha 6$ -null pericytes. Bar chart represents % adhesion of pericytes to Lm-1 relative to adhesion to Fn for the same genotype. n=3 biological repeats; **p<0.01. Sections from tumours grown in *pdgfr β cre-; $\alpha 6$ fl/fl* and *pdgfr β cre+; $\alpha 6$ fl/fl* mice were stained with antibodies to inflammatory cell markers **(B)** CD8 (T cells), **(C)** CD45 cells and **(D)** F480 (macrophages). No difference in inflammatory cell infiltration was observed between tumours from either genotype. Bar charts represent % immune cell infiltration; n=6 tumours/genotype; ns= not significantly different. Scale bar =100 μ m.



Supplementary Figure 4. Characterisation of primary mouse brain pericytes, primary mouse lung endothelial cells and fibroblasts and Reverse Phase Protein Array (RPPA) analysis reveals the mTOR signalling pathway is attenuated in α 6-null mouse brain

pericytes. (A) Primary mouse brain pericytes were characterised using the following markers, by FACS: PDGFR β , CD146, CD31 (endothelial marker), glial fibrillary acidic protein (GFAP) and Mac1 (fibroblast markers). Red graph = unstained cells, blue graph = stained cells. The results are shown as a histogram (left) and dot plot (right). *pdgfr β cre-; α 6fl/fl* mouse brain pericytes were also immunostained for NG2 (pericyte marker) and visualised by epifluorescence microscopy. (B) Primary mouse lung endothelial cells were stained for CD31 followed by FACS analysis and immunostained for endomucin and vimentin (expressed by ECs) and α -sma (fibroblast marker). (C) Primary mouse lung fibroblasts were immunostained for vimentin (positive marker for fibroblasts), NG2 and endomucin (negative markers for fibroblasts). Rat IgG was used as a negative control. (D) RPPA analysis of protein extracted from WT and α 6-null pericytes showed a significant reduction in many proteins in α 6-null pericytes. These included components of the mTOR signalling pathway – AKT, p70S6kinase, mTOR, pS6 ribosomal protein and 4E-BP1; this pathway is important for several cell functions including growth, migration, proliferation and angiogenesis and is known to be activated by integrins.